

# Heisenberg model with Dzyaloshinskii-Moriya interaction: A mean-field Schwinger boson study

L. O. Manuel, C. J. Gazza, A. E. Trumper,  
and H. A. Ceccatto

*Instituto de Física Rosario, Universidad Nacional de Rosario  
and Consejo Nacional de Investigaciones Científicas y Técnicas,  
Boulevard 27 de Febrero 210 Bis, 2000 Rosario, República Argentina*

We present a Schwinger-boson approach to the Heisenberg model with Dzyaloshinskii-Moriya interaction. We write the anisotropic interactions in terms of Schwinger bosons keeping the correct symmetries present in the spin representation, which allows us to perform a conserving mean-field approximation. Unlike previous studies of this model by linear spin-wave theory, our approach takes into account magnon-magnon interactions and includes the effects of three-boson terms characteristic of noncollinear phases. The results reproduce the linear spin-wave predictions in the semiclassical large- $S$  limit, and show a small renormalization in the strong quantum limit  $S = 1/2$ .

For the sake of definiteness, we specialize the calculations for the pattern of Moriya vectors corresponding to the orthorhombic phase in  $\text{La}_2\text{CuO}_4$ , and give a fairly detailed account of the behavior of ground-state energy, anisotropy gap, and net ferromagnetic moment. In the last part of this work we generalize our approach to describe the geometry of the intermediate phase in  $\text{La}_{2-x}\text{Nd}_x\text{CuO}_4$ , and discuss the effects of including nondegenerate  $2p_z$  oxygen orbitals in the calculations.

## I. INTRODUCTION

Dzyaloshinskii [1] was the first to point out that weak ferromagnetism in antiferromagnetic compounds can be explained by an antisymmetric spin-spin interaction. The microscopic basis for this theory was later given by Moriya, [2] who extended Anderson's superexchange theory [3] to include the spin-orbit interactions. He considered that only the antisymmetric part of the anisotropic spin-spin interactions he derived was relevant because it is linear in the spin-orbit coupling, while the symmetric anisotropies are of second order. However, in a recent work Shekhtman *et al.* [4] showed that the symmetric anisotropic term cannot be neglected, and that the whole two-spin anisotropic interaction can be mapped onto the isotropic Heisenberg interaction by a bond-depending rotation of the original spins. This surprising result means that the anisotropy coming from the spin-orbit coupling does not lift by itself the ground-state degeneracy, unless the required local transformations to map the entire Hamiltonian to the isotropic one are not all consistent. Using the mapping to the isotropic model these authors showed that infinitely many states with different ferromagnetic moments are degenerate with the purely antiferromagnetic one. Then, they concluded that some kind of frustration of the required local transformations is a necessary ingredient to have a definite ferromagnetic moment in the ground-state, a condition that had been previously overlooked.

The results of Ref. [4] are relevant to explain the small ferromagnetic moment observed in the  $\text{CuO}_2$  planes of undoped  $\text{La}_2\text{CuO}_4$ . [5] This compound undergoes a structural phase transition from tetragonal to orthorhombic symmetry at  $T \simeq 500$  K. [6] In the orthorhombic phase the  $\text{CuO}_6$  octahedra forming each  $\text{CuO}$  layer tilt in a staggered pattern about the  $\langle 110 \rangle$  axis, and this distortion combined with the Dzyaloshinskii-Moriya (DM) interactions induces a weak ferromagnetic moment in each layer. Coffey *et al.* [7,8] determined the DM vectors in both phases from symmetry analysis and detailed microscopic calculations. They emphasized that the existence of a net ferromagnetic moment requires an alternating pattern of Moriya vectors that change in sign from one bond to the next. However, only the consideration of the hidden symmetry discussed in [4] allows one to show that only for the orthorhombic symmetries the corresponding pattern leads to the observed small ferromagnetic moment, while those of the tetragonal phase do not allow it. These results were later generalized by Bonesteel [9] to describe the intermediate phase observed in  $\text{La}_{2-x}\text{Nd}_x\text{CuO}_4$ , where the oxygen octahedra rotate around a general axis in the  $\text{CuO}_2$  plane. [10]

In this work we focus on the study of the Heisenberg Hamiltonian with DM interaction in the strong quantum limit  $S = 1/2$ . The same Hamiltonian was previously studied by semiclassical linear spin-wave theory in Refs. [9,11], with the emphasis put on magnon dispersion relations. However, since the classical ground state is not collinear, relevant three-boson terms coming from the Holstein-Primakoff representation of spins have been ignored. In this case we extend the Schwinger-boson theory discussed in [12] to consider the anisotropic DM terms, and include magnon-magnon interactions in a saddle-point evaluation of the resulting bosonic Hamiltonian. We give a fairly detailed account of the energy, ferromagnetic moment, and gap behaviors as a function of the size and relative orientation of Moriya vectors, and compare these results with similar predictions from linear spin-wave theory. We will first specialize the calculations for the pattern of microscopic Moriya vectors

corresponding to the orthorhombic phase in  $\text{La}_2\text{CuO}_4$ . Then, in the last part of this work, we will generalize our approach to describe the intermediate phase in  $\text{La}_{2-x}\text{Nd}_x\text{CuO}_4$ .

The layout of this work is as follows. In Sec. 2 we discuss the representation by Schwinger bosons of the anisotropic terms coming from the DM interaction. In Sec. 3 we describe the classical ground state of the model, and interpret its structure as a spiral order in a topologically-equivalent decorated lattice. This allows us to make contact with the theory developed in [12]. In Sec. 4 we sketch the calculation of quantum fluctuations above this classical ground state. We give here explicit expressions in terms of the order parameters for the quasiparticle dispersion relation, ground-state energy, etc. In Sec. 5 we solve numerically the consistency equations and present the results for relevant quantities. In addition, in Sec. 6 we generalize the calculations to describe the intermediate phase in  $\text{La}_{2-x}\text{Nd}_x\text{CuO}_4$  and discuss the effects of including the oxygen  $2p_z$  orbitals. [11,13] Finally, we end up with some conclusions.

## II. BOSON REPRESENTATION OF THE DZIALOSHINSKII-MORIYA INTERACTION

In its simplest derivation, [2] the Heisenberg Hamiltonian including the DM interaction can be obtained starting from the one-electron Hamiltonian

$$H_{1-el} = \sum_{i,\sigma} \epsilon_i c_{i\sigma}^\dagger c_{i\sigma} + \sum_{\langle ij \rangle, \sigma\sigma'} c_{i\sigma}^\dagger (t e^{i\theta \hat{\mathbf{d}}_{ij} \cdot \boldsymbol{\sigma}})_{\sigma\sigma'} c_{j\sigma'} , \quad (1)$$

where  $i, j$  are nearest neighbor sites, and the term nondiagonal in spin space takes into account the spin-orbit interaction. We assume nondegenerate ground-state orbitals, and  $t$  and  $\theta$  are taken independent of the bond  $\langle ij \rangle$  for simplicity. The unit vector  $\hat{\mathbf{d}}_{ij} = -\hat{\mathbf{d}}_{ji}$ . Then, by using second-order perturbation theory in the presence of an on-site repulsion  $U$  [3] one obtains the interaction between spins at sites  $i, j$  as

$$E_{ij} = J \mathbf{S}_i \cdot \mathbf{S}_j + \mathbf{D}_{ij}^M \cdot (\mathbf{S}_i \times \mathbf{S}_j) + \mathbf{S}_i \cdot \Gamma_{ij} \cdot \mathbf{S}_j . \quad (2)$$

In this expression the superexchange interaction  $J = (4t^2/U) \cos^2 \theta$ . The last two terms of (2) are the contributions coming from the spin-orbit interaction of the original electrons. They contain the antisymmetric Moriya vector  $\mathbf{D}_{ij}^M = 2Jr\hat{\mathbf{d}}_{ij}$  ( $r = \tan \theta$ ), and the symmetric anisotropy tensor  $\Gamma$ . In fact, (2) can be most simply written as [4]

$$\begin{aligned} E_{ij} &= J \left( \mathbf{S}_i \cdot \mathbf{S}_j + 2r\hat{\mathbf{d}}_{ij} \cdot (\mathbf{S}_i \times \mathbf{S}_j) + r^2 \left[ 2(\hat{\mathbf{d}}_{ij} \cdot \mathbf{S}_i)(\hat{\mathbf{d}}_{ij} \cdot \mathbf{S}_j) - \mathbf{S}_i \cdot \mathbf{S}_j \right] \right) \\ &= J_0 \mathbf{S}'_i \cdot \mathbf{S}'_j , \end{aligned} \quad (3)$$

where  $J_0 = 4t^2/U$ . The spins  $\mathbf{S}'_i, \mathbf{S}'_j$  are obtained by rotating the original ones around the  $\hat{\mathbf{d}}_{ij}$  axis:

$$\mathbf{S}'_k = (1 - \cos \theta_k)(\hat{\mathbf{d}}_{ij} \cdot \mathbf{S}_k)\hat{\mathbf{d}}_{ij} + \cos \theta_k \mathbf{S}_k - \sin \theta_k \mathbf{S}_k \times \hat{\mathbf{d}}_{ij} \quad (k = i, j) , \quad (4)$$

with the rotation angles given by  $\theta_i = \theta = -\theta_j$ .

At this point we introduce the Schwinger representation  $\mathbf{S}' = \mathbf{a}'^\dagger \cdot \sigma \cdot \mathbf{a}'$ , where the bosonic spinor  $\mathbf{a}'^\dagger \equiv (a_{\uparrow}'^\dagger, a_{\downarrow}'^\dagger)$ . Then, the rotational invariant structure in (3) can be written in the usual way [12] as

$$\mathbf{S}'_i \cdot \mathbf{S}'_j =: B_{ij}^\dagger B'_{ij} : - A_{ij}^\dagger A'_{ij} , \quad (5)$$

in terms of the  $SU(2)$  singlets

$$B_{ij}^\dagger = \frac{1}{2} \sum_{\sigma} a_{i\sigma}^\dagger a'_{j\sigma} , \quad A'_{ij} = \frac{1}{2} \sum_{\sigma} \sigma a'_{i\sigma} a'_{j,-\sigma} .$$

In (5) the colons denote a normal-ordered product of Bose operators.

From standard rotation properties we have:

$$\mathbf{S}' = \mathcal{R}_\theta \mathbf{S} = \mathbf{a}^\dagger \cdot (\mathcal{R}_\theta \sigma) \cdot \mathbf{a} = (\mathbf{a}^\dagger \mathcal{U}_\theta^\dagger) \cdot \sigma \cdot (\mathcal{U}_\theta \mathbf{a}) = \mathbf{a}'^\dagger \cdot \sigma \cdot \mathbf{a}' ,$$

where  $\mathcal{R}_\theta$  is the three-dimensional matrix that rotates an angle  $\theta$  around the  $\hat{\mathbf{d}}_{ij}$  axis, and  $\mathcal{U}_\theta = \exp[-i(\theta/2)\hat{\mathbf{d}}_{ij} \cdot \sigma]$  is the corresponding  $SU(2)$  matrix. In this way we have  $\mathbf{a}' = \mathcal{U}_\theta \mathbf{a}$ , and this relation can be replaced in the definitions of the  $A', B'$  singlets in order to express them in terms of the unrotated spinors:

$$B_{ij}^\dagger = \cos \theta B_{ij}^\dagger + \sin \theta C_{ij}^\dagger , \quad A'_{ij} = \cos \theta A_{ij} - \sin \theta D_{ij} . \quad (6)$$

Here, in addition to the singlets  $A, B$  we have defined

$$C_{ij}^\dagger = \frac{1}{2} \sum_{\sigma\sigma'} a_{i\sigma}^\dagger (i\hat{\mathbf{d}}_{ij} \cdot \sigma)_{\sigma\sigma'} a_{j\sigma'} , \quad D_{ij} = \frac{1}{2} \sum_{\sigma,\sigma'} a_{i\sigma} (\sigma^y \hat{\mathbf{d}}_{ij} \cdot \sigma)_{\sigma\sigma'} a_{j\sigma'} .$$

By replacing (5),(6) in (3) we can identify the correct expressions in terms of Schwinger bosons of the spin interactions:

$$\begin{aligned} \mathbf{S}_i \cdot \mathbf{S}_j &=: B_{ij}^\dagger B_{ij} : - A_{ij}^\dagger A_{ij} \\ \hat{\mathbf{d}}_{ij} \cdot (\mathbf{S}_i \times \mathbf{S}_j) &= \frac{1}{2} (: B_{ij}^\dagger C_{ij} + C_{ij}^\dagger B_{ij} : + A_{ij}^\dagger D_{ij} + D_{ij}^\dagger A_{ij} ) \end{aligned} \quad (7)$$

$$2(\hat{\mathbf{d}}_{ij} \cdot \mathbf{S}_i)(\hat{\mathbf{d}}_{ij} \cdot \mathbf{S}_j) - \mathbf{S}_i \cdot \mathbf{S}_j =: C_{ij}^\dagger C_{ij} : - D_{ij}^\dagger D_{ij} .$$

In this way the DM terms are given as products of bilinear boson operators that have the same rotational properties of the original spin interactions. This allows us to perform a conserving mean-field approximation by breaking these products. However, before undertaking the study of the resulting mean-field Hamiltonian, in the next section we specialize the above results for the  $\text{CuO}_2$  planes in the low-temperature orthorhombic (LTO) phase of  $\text{La}_2\text{CuO}_4$ , and discuss how to describe the structure of the corresponding classical ground states as commensurate spiral orders.

### III. THE CLASSICAL GROUND STATE AS A SPIRAL ORDER

If the rotations required at every site to bring the spin-spin interactions for *all* bonds in the lattice to the form (3) are compatible, then the Hamiltonian  $H_{spin} = (1/2) \sum_{\langle ij \rangle} E_{ij}$  is isomorphic to the isotropic Heisenberg model. This happens when the product of the four rotations around each basic plaquette in the lattice equals unity, which corresponds to the *unfrustrated* case. In this case, in correspondence with the ground-state degeneracy of (3) there is also a large degeneracy in the ground state of  $H_{spin}$ . From the relations (4) between original and rotated spins we see that by judiciously choosing the direction of the Néel we can find ground states of  $H_{spin}$  with no net ferromagnetic moment ( $\mathbf{S}'_i = -\mathbf{S}'_j$  parallel to  $\hat{\mathbf{d}}_{ij}$ ) up to a maximum ferromagnetic moment of  $\pm \sin \theta$  ( $\mathbf{S}'_i = -\mathbf{S}'_j$  perpendicular to  $\hat{\mathbf{d}}_{ij}$ ). Even though  $\mathbf{D}_{ij}^M$  in (2) points in a special direction in spin space, because of the presence of the symmetric tensor  $\Gamma$  this anisotropy does not lift the degeneracy of the ground state. [4]

According to the above discussion, in order to have a net ferromagnetic moment there should be some degree of *frustration* in the system. [4] That is, there should exist no spin rotations that map the entire Hamiltonian onto an isotropic one. In particular, in the LTO phase of  $\text{La}_2\text{CuO}_4$  the crystal structure leads to the pattern of Moriya vectors shown in Fig. 1. In this figure  $\mathbf{D}_1 = D\hat{\mathbf{d}}_1$  and  $\mathbf{D}_2 = D\hat{\mathbf{d}}_2$ , where  $\hat{\mathbf{d}}_1 = (\sin \beta, \cos \beta, 0)$ ,  $\hat{\mathbf{d}}_2 = (\cos \beta, \sin \beta, 0)$ , and  $D = 2Jr$  as in the previous section [14]. Then, the magnetic structure can be described in terms of two interpenetrating sublattices. Defining  $\mathbf{D}^\pm = (\mathbf{D}_1 \pm \mathbf{D}_2)/2$ , it has been shown [15] that the system develops a net ferromagnetic moment only when both  $\mathbf{D}^-$  and  $\mathbf{D}^+$  are different from zero ( $\beta \neq \pm\pi/4$ ). In such a case the staggered magnetization of the ground state is directed along  $\mathbf{D}^-$ , and the ferromagnetic moment is proportional to  $\mathbf{D}^+ \times \mathbf{D}^-$  (see Fig. 2).

In the two-sublattice picture the classical ground state has magnetizations  $\mathbf{S}_A = (S \cos \phi, 0, S \sin \phi)$  and  $\mathbf{S}_B = (-S \cos \phi, 0, S \sin \phi)$ , with  $\tan \phi = r \cos(\beta - \pi/4)$  (We are using the  $x$ -axis in spin space directed along  $\mathbf{D}^-$  and the  $z$ -axis perpendicular to the  $\text{CuO}_2$  plane). In order to make contact with the theory developed in [12] it is convenient to describe this state as a commensurate spiral order in a distorted lattice. To this end we move the sites belonging to sublattices  $A, B$  by vectors  $\vec{\delta}_A = (\phi/\pi, 0)$  and  $\vec{\delta}_B = -\vec{\delta}_A$  respectively (see Fig. 3), so that the basis vectors of the new decorated square lattice are  $\vec{\delta}_A$  and  $\vec{\delta}_1 = (1, 0) + \vec{\delta}_B$  (We took the original lattice constant  $a = 1$  and used arrows instead of boldface to indicate vectors in real space). The magnetic order is then given by  $\mathbf{S}_{\vec{r}} = (S \cos \vec{Q} \cdot \vec{r}, 0, S \sin \vec{Q} \cdot \vec{r})$ , where the magnetic wavevector  $\vec{Q} = (\pi, \pi)$  and the  $\vec{r}$ 's indicate the sites of the distorted lattice. This classical ground state can be described by condensing the Schwinger bosons according to  $a_{\vec{r}\sigma}^\dagger = a_{\vec{r}\sigma} = \sqrt{S}(\cos \vec{Q} \cdot \vec{r}/2 + \sigma \sin \vec{Q} \cdot \vec{r}/2)$ . In the next section we will incorporate the quantum fluctuations on this description by considering the Schwinger-boson dynamics to mean-field order.

### IV. QUANTUM DESCRIPTION TO MEAN-FIELD ORDER

Once  $H_{spin}$  is expressed in terms of Schwinger bosons as indicated in Sec. 2 (see (7)), all the four-boson products are decoupled using as order parameters the mean values of the correlations  $A, B, C, D$  between sites in different sublattices. Then, the mean-field Hamiltonian

becomes:

$$H_{\text{MF}} = \sum_{i, \vec{\delta}} [\mathcal{B}(\vec{\delta}) \mathcal{B}_{i, i+\vec{\delta}}^\dagger - \mathcal{A}(\vec{\delta}) \mathcal{A}_{i, i+\vec{\delta}}^\dagger + \text{H.c.}] - N \sum_{\vec{\delta}} (|\mathcal{B}(\vec{\delta})|^2 - |\mathcal{A}(\vec{\delta})|^2), \quad (8)$$

where  $\mathcal{B}_{i, i+\vec{\delta}} \equiv B_{i, i+\vec{\delta}} + rC_{i, i+\vec{\delta}}$ ,  $\mathcal{A}_{i, i+\vec{\delta}} \equiv A_{i, i+\vec{\delta}} - rD_{i, i+\vec{\delta}}$ , and  $\mathcal{B}(\vec{\delta}), \mathcal{A}(\vec{\delta})$  are their corresponding mean-field values. Here  $N$  is the number of decorated unit cells and  $i$  runs on the  $A$  sublattice. In particular, because of the geometry of Moriya vectors in Fig. 1, the  $C, D$  operators take the simple form

$$C_{i, i+\vec{\delta}}^\dagger = \frac{1}{2} \sum_{\sigma} \sigma e^{i\sigma\eta(\vec{\delta})} a_{i\sigma}^\dagger a_{i+\vec{\delta}, -\sigma}, \quad D_{i, i+\vec{\delta}} = \frac{1}{2} \sum_{\sigma} e^{-i\sigma\eta(\vec{\delta})} a_{i\sigma} a_{i+\vec{\delta}, \sigma},$$

with  $\eta(\vec{\delta}_j) = (-)^j(\pi/4 - \beta)$  ( $j = 1, 4$ ).

We perform now a transformation to reciprocal space according to

$$a_{i\sigma} = \frac{1}{\sqrt{N}} \sum_{\vec{k}} \alpha_{\vec{k}\sigma} e^{-i\vec{k}\sigma \cdot \vec{r}_i}, \quad a_{i+\vec{\delta}, \sigma} = \frac{1}{\sqrt{N}} \sum_{\vec{k}} \beta_{\vec{k}\sigma} e^{-i\vec{k}\sigma \cdot \vec{r}_{i+\vec{\delta}}},$$

where  $\vec{k}_\sigma = \vec{k} + \sigma\vec{Q}/2$  and the  $\vec{k}$ 's are the normal modes of the decorated lattice. The resulting Hamiltonian has to be supplemented by adding, through Lagrange multipliers  $\lambda_A, \lambda_B$ , the restrictions on the number of bosons on each sublattice:

$$\sum_{\vec{k}\sigma} \langle \alpha_{\vec{k}\sigma}^\dagger \alpha_{\vec{k}\sigma} \rangle = 2SN, \quad \sum_{\vec{k}\sigma} \langle \beta_{\vec{k}\sigma}^\dagger \beta_{\vec{k}\sigma} \rangle = 2SN.$$

Notice, however, that these restrictions are only the average of the exact constraints *per site* required to have a faithful representation of the spin algebra. With this simplification we obtain a  $8 \times 8$  dynamical matrix which has to be diagonalized numerically. However, the solution of the mean-field equations for the  $\mathcal{A}, \mathcal{B}$  order parameters shows that, for the symmetry of the spiral order, the parameters  $\mathcal{B}(\vec{\delta}) = 0$  and  $\lambda_A = \lambda_B$ . Then, the original dynamical matrix decouples in two  $4 \times 4$  blocks given by:

$$\Delta(\vec{q}) = \begin{pmatrix} \lambda & 0 & -\gamma(\vec{q}) & \gamma_+(\vec{q}) \\ 0 & \lambda & \gamma_-(\vec{q}) & \gamma(\vec{q}) \\ -\gamma^*(\vec{q}) & \gamma_-^*(\vec{q}) & \lambda & 0 \\ \gamma_+^*(\vec{q}) & \gamma^*(\vec{q}) & 0 & \lambda \end{pmatrix} \quad (9)$$

and the corresponding one with  $\vec{q} \equiv \vec{k} + \vec{Q}/2$  replaced by  $-\vec{q}$ . We have defined:

$$\gamma(\vec{q}) = \frac{1}{2} \sum_{\vec{\delta}} \mathcal{A}(\vec{\delta}) e^{-i\vec{q} \cdot (\vec{\delta} - \vec{\delta}_A)}, \quad \gamma_{\pm}(\vec{q}) = \frac{1}{2} \sum_{\vec{\delta}} r \mathcal{A}(\vec{\delta}) e^{-i\vec{q} \cdot (\vec{\delta} - \vec{\delta}_A) \pm i\eta(\vec{\delta})}.$$

Paraunitary diagonalization of (9) produces the quasiparticle dispersion relations

$$\omega_{\pm}^2 = \lambda^2 - \left( |\gamma|^2 + \frac{1}{2} (|\gamma_+|^2 + |\gamma_-|^2) \right) \pm \sqrt{\frac{1}{4} (|\gamma_+|^2 - |\gamma_-|^2)^2 + |\gamma^* \gamma_+ - \gamma \gamma_-|^2}.$$

Numerical evaluation (see next section) shows that the in-plane and out-of-plane gaps are degenerate. For the unfrustrated case  $\beta = \pi/4$ , so that  $\gamma_{\pm} = \gamma$ , and this equation reduces to  $\omega_{\pm}^2 = \lambda^2 - (1 + r^2)|\gamma|^2$ . As expected, these degenerate quasiparticle bands correspond to an antiferromagnet with renormalized interaction  $J(1 + r^2) = J/\cos^2 \theta \equiv J_0$  (see (3)).

The ground-state energy is given by  $E_0 = (1/2) \sum_{\vec{k}\sigma} \omega_{\sigma}(\vec{k}) - (2S+1)N\lambda$ . The mean-field equations that determine the parameters  $\lambda$  and  $\mathcal{A}(\delta)$  are obtained by minimization of  $E_0$ . In the next section we discuss the results obtained by solving numerically these equations.

## V. RESULTS FOR THE LTO PHASE OF $\text{La}_2\text{CuO}_4$

We have solved numerically the consistency equations by iteration, starting from the classical values of the order parameters and Lagrange multiplier (The classical values of the order parameters can be obtained by using the structure of the boson condensate given at the end of Sec. 3, and  $\lambda_{cl} = -E_{cl}/NS^2 = 2(1 + r^2)$ ). For the unfrustrated case  $\beta = \pi/4$  we obtain, as expected, two doubly-degenerate quasiparticles branches corresponding to an isotropic antiferromagnet with the effective coupling  $J_0$ . For  $\beta$  infinitesimally smaller than  $\pi/4$  one of these branches develops gaps at  $\vec{k} = \vec{0}$ , which correspond to the degenerate in- and out-of-plane gaps associated to the anisotropy. The other branch remains very much unaffected, i.e., almost identical to the isotropic renormalized antiferromagnetic dispersion. For large  $S$  the gapped branch becomes the linear spin-wave dispersion relation. [9,11] In Fig. 4 we plot both branches for  $\beta = 0$  and  $r = 0.4$  along the typical  $(\Gamma, X, M)$  path there indicated. The dashed line gives the results of linear spin-wave theory for comparison. The fact that one of the branches remain gapless can be understood by noticing that in the Schwinger-boson approach the existence of a local magnetization is intimately linked to the boson condensation. Then, in order for the system to have a magnetized ground state, the chemical potential (Lagrange multiplier) must be pinned to the bottom of one of the original boson bands, giving a gapless quasiparticle branch. This can be confirmed by simply studying the isotropic antiferromagnet with a staggered magnetic field. On the other hand, from a physical point of view this is not a problem since the exact form of the constraint requires creation and destruction of both kind of quasiparticles to describe a magnon. In Fig. 5 we plot the gap as a function of  $r$  for  $\beta = 0$  [16]. Notice that for the physical value  $r \simeq 0.1$  the result is indistinguishable from the spin wave prediction.

The classical energy is given by  $E_{cl} = -2(1 + r^2)$ , and is independent of the frustration. In Fig. 6 we plot the ratio between the quantum and classical ground-state energies as a function of  $\beta$  for several values of  $r$ . As can be seen, quantum fluctuations are sensitive to the degree of frustration, although the changes in energy are not important even for unphysically large values of  $r$ . In Fig. 7 we plot the behavior of the net ferromagnetic moment for the same values of  $r$ . As expected, [15] it goes to zero for  $\beta = -\pi/4$ , where the Dzyaloshinskii vector  $\mathbf{D}^+$  vanishes and the ground-state configuration is completely antiferromagnetic (see Sec. 3). The values at  $\beta = \pi/4$  correspond to the ferromagnetic moments in the unfrustrated case ( $\mathbf{D}^- = 0$ ). However, these moments are unobservable since, as pointed out above, in this case the Hamiltonian becomes isomorphic to the isotropic Heisenberg model. [4] Notice that this happens only exactly at  $\beta = \pi/4$ ; for slightly different values the system develops a relatively large net ferromagnetic moment. Notably, as shown in Fig. 7 in the quantum case

the maximum ferromagnetic moment is obtained for some intermediate value of  $\beta$  which depends weakly on  $r$ .

## VI. INTERMEDIATE PHASE IN $\text{La}_{2-x}\text{Nd}_x\text{CuO}_4$

In the LTO phase the  $\text{CuO}_6$  octahedra forming each CuO layer tilt in a staggered pattern about the  $\langle 110 \rangle$  axis. In this section we consider the effects of DM interactions which occur in the presence of tilting distortions about an arbitrary axis. Such general tilting distortions may have physical relevance for  $\text{La}_{2-x}\text{Nd}_x\text{CuO}_4$ . [9]

In order to generalize the above calculations for an arbitrary direction of the octahedra tilting axis we have to perform the following changes: i) In Sec. 2, the parameters  $t$  and  $\theta$  of (1) must be bond dependent, which implies that  $|D_{ij}^M|$  is also bond dependent; ii) In Sec. 3, the new pattern of Moriya vectors is given by  $\mathbf{D}_1 = (\lambda_1 \cos \alpha, \lambda_2 \sin \alpha, 0)$  and  $\mathbf{D}_2 = (\lambda_2 \cos \alpha, \lambda_1 \sin \alpha, 0)$ , with  $\alpha$  the angle between the octahedra rotation axis and the  $[100]$  direction in the CuO plane, and  $\lambda_1 \simeq 0$  [9] (The angle  $\alpha$  equals zero in the tetragonal phase and  $\pi/4$  in the orthorhombic phase). Furthermore, the angle  $\phi$  which characterizes the classical ground-state spin configuration satisfies  $\sin \phi = \sin \psi \sin 2\alpha$ , where  $\tan \psi = \lambda_2/2J$  [11]; iv) In Sec. 4, the parameter  $r = |D_{ij}^M|/2J$  is now bond dependent. This leads to different  $\mathcal{A}(\vec{\delta})$  for each bond direction, but  $\mathcal{B}(\vec{\delta})$  remains zero and the dispersion relations have the same formal expression. With these changes we obtained the following results: The ground-state energy and gap depend slightly on the tilting axis angle  $\alpha$ . On the contrary, the net ferromagnetic moment is strongly dependent on  $\alpha$  (see Fig. 8). It vanishes in the tetragonal phase ( $\alpha = 0$ ) and reaches its maximum value in the LTO phase ( $\alpha = \pi/4$ ).

In [13] it has been suggested that the inclusion of the oxygen  $2p_z$  orbitals would account for the weak ferromagnetism in the LTO phase of  $\text{La}_2\text{CuO}_4$ , with the frustration origin advocated in [4] being irrelevant. However, Entin-Wohlman *et al.* [11] showed that the effects of introducing these orbitals is too small to be responsible for the observed weak ferromagnetism. On the other hand, the multilevel mechanism does break the degeneracy of the in- and out-of-plane gaps, although the relative magnitude of this breaking is again too small when compared to experiments. We have also considered including the  $2p_z$  orbitals in our calculations. In this case the required changes are the following: i) In Sec. 2, Eq. (3) has to be replaced by

$$E_{ij} = J\mathbf{S}_i \cdot \mathbf{S}_j + \mathbf{D}_{ij} \cdot (\mathbf{S}_i \times \mathbf{S}_j) + \frac{1}{4J}(1 - \Omega) \left[ 2(\mathbf{D}_{ij} \cdot \mathbf{S}_i)(\mathbf{D}_{ij} \cdot \mathbf{S}_j) - |D_{ij}|^2 \mathbf{S}_i \cdot \mathbf{S}_j \right],$$

where  $\Omega$  is proportional to the energy difference between the  $2p_z$  and  $2p_\sigma$  orbitals of the oxygen [11]; ii) In Sec. 3, the angle  $\phi$  that describes the classical ground state has a complex expression in terms of the parameters of the model. We have obtained it by numerical minimization of the classical energy; iii) In Sec. 4, the mean-field Hamiltonian (8) has to be written as a function of the four order parameters  $A, B, C$  and  $D$ . The  $8 \times 8$  dynamical matrix no longer decouples in two blocks, so that its paraunitary diagonalization has to be performed numerically. In Fig. 9 we present the new dispersion relations obtained in this case, for  $\lambda_1 = 0$ ,  $\lambda_2 = 0.6$ ,  $\alpha = \pi/8$ , and  $\Omega = 0.4$ . As can be seen, the degenerate gapped branch splits into two branches that differ mostly near the gap wavevector. However, even for this large  $\Omega$  the ratio between the in- and out-of-plane gaps is still much smaller than



the experimental value. Finally, in Fig. 10 we plot the ferromagnetic moment for different values of  $\Omega$ . Remarkably, for some special value of  $\alpha$  this moment becomes independent of  $\Omega$ .

## VII. CONCLUSIONS

We presented a Schwinger-boson approach to the Heisenberg model with DM interaction. We showed how to represent the anisotropic DM interactions in terms of Schwinger bosons keeping the correct symmetries present in the spin representation, which allowed us to perform a conserving mean-field approximation. Unlike previous studies of this model by linear spin-wave theory, our approach takes into account magnon-magnon interactions already at mean-field order and includes the effects of three-boson terms, characteristic of noncollinear phases, which are ignored in standard studies. Our results recover the linear spin-wave predictions in the semiclassical large- $S$  limit, and show a small renormalization in the strong quantum limit  $S = 1/2$ .

Although the emphasis was put on the basic properties of the model Hamiltonian studied, for definiteness we considered a pattern of Moriya vectors corresponding to the LTO phase in  $\text{La}_2\text{CuO}_4$ . In the last section we generalized the calculations to discuss the behavior of relevant quantities for arbitrary directions of the octahedra tilting axis, which might be relevant to describe the intermediate phase in  $\text{La}_{2-x}\text{Nd}_x\text{CuO}_4$ . Finally, we have also considered the inclusion of nondegenerate  $2p_z$  oxygen orbitals, and showed that they cannot account for the experimentally observed difference between in- and out-of-plane gaps.

- 
- [1] I. E. Dzyaloshinski, J. Chem. Solids **4**, 241 (1958).
  - [2] T. Moriya, Phys. Rev. **120**, 91 (1960); *ibid*, Phys. Rev. Lett. **4**, 228 (1960).
  - [3] P.W. Anderson, Phys. Rev. **115**, 2 (1959).
  - [4] L. Shekhtman, O. Entin-Wohlman, and Amnon Aharony, Phys. Rev. Lett. **69**, 836 (1992).
  - [5] S.W. Cheong, J.D. Thompson, and Z. Fisk, Phys. Rev. B **39**, 4395 (1989).
  - [6] J.D. Jorgensen, *et al.*, Phys. Rev. B **38**, 11337 (1988), and references therein.
  - [7] D. Coffey, K.S. Bedell, and S.A. Trugman, Phys. Rev. B **42**, 6509 (1990)
  - [8] D. Coffey, T.M. Rice, and F.C. Zhang, Phys. Rev. B **44**, 10112 (1991); *ibid.* **46**, 5884 (E) (1992)
  - [9] N.E. Bonesteel, Phys. Rev. B **47**, 11302 (1993).
  - [10] M. Crawford *et al.*, Phys. Rev. B **44**, 7749 (1991).
  - [11] O. Entin-Wohlman, Amnon Aharony, and L. Shekhtman, Phys. Rev. B **50**, 3068 (1994).
  - [12] H.A. Ceccatto, C.J. Gazza, and A.E. Trumper, Phys. Rev. B **47**, 12329 (1993).
  - [13] W. Koshibae, Y. Ohta, and S. Maekawa, Phys. Rev. B **47**, 3391 (1993); **48**, 3580 (E) (1993).
  - [14] For generality we will consider the behavior of relevant quantities for arbitrary values of  $\beta$ , although it is in fact almost zero [8]. Notice that because of the symmetries it is only necessary to consider  $-\pi/4 \leq \beta \leq \pi/4$ .
  - [15] L. Shekhtman, Amnon Aharony, and O. Entin-Wohlman, Phys. Rev. B **47**, 174 (1993).

[16] The physical values in the LTO phase of  $\text{La}_2\text{CuO}_4$  are  $\beta \simeq 0$  and  $r \simeq 0.1$  [17]. We are considering a larger value of  $r$  in order to emphasize the presence of a gap in this figure.

[17] T. Thio *et al.*, Phys. Rev. B **38**, 905 (1988).

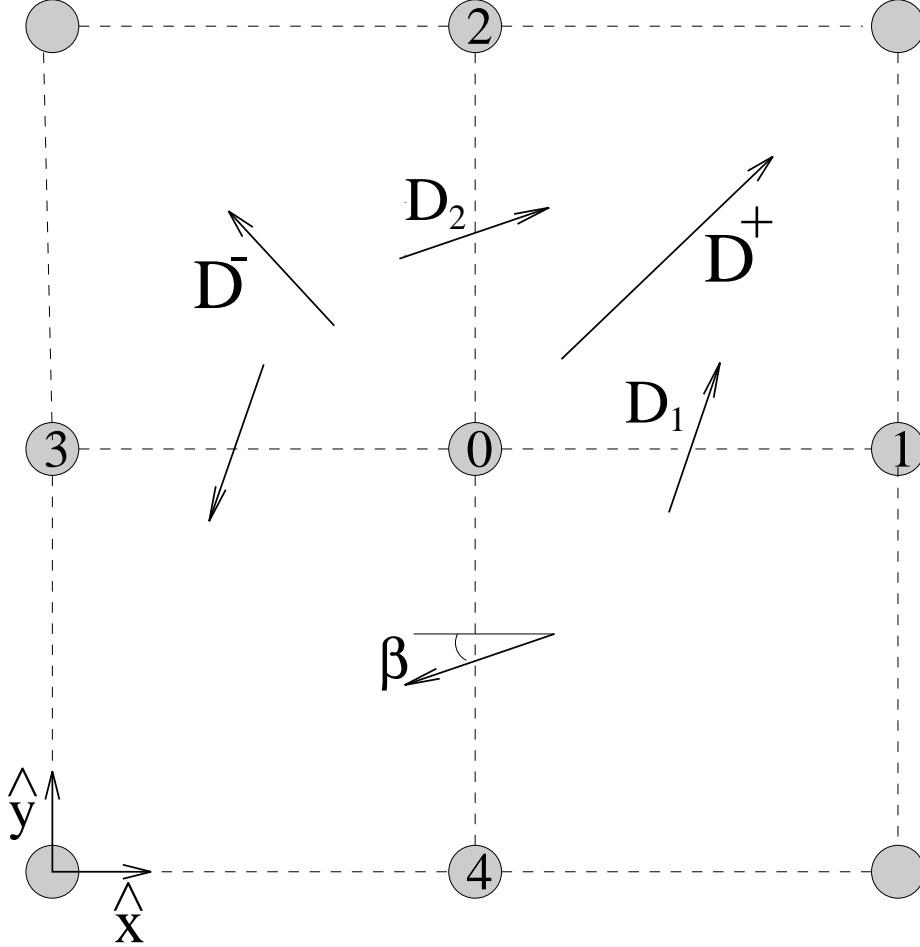


FIG. 1. Copper sites of the  $\text{CuO}_2$  planes in  $\text{La}_2\text{CuO}_4$ . We indicate the bond-dependent Moriya vectors  $\mathbf{D}_{ij}^M$ , which alternate in sign along the  $x$  and  $y$  axis. Also shown are the corresponding  $\mathbf{D}^\pm$  vectors defined in the main text.

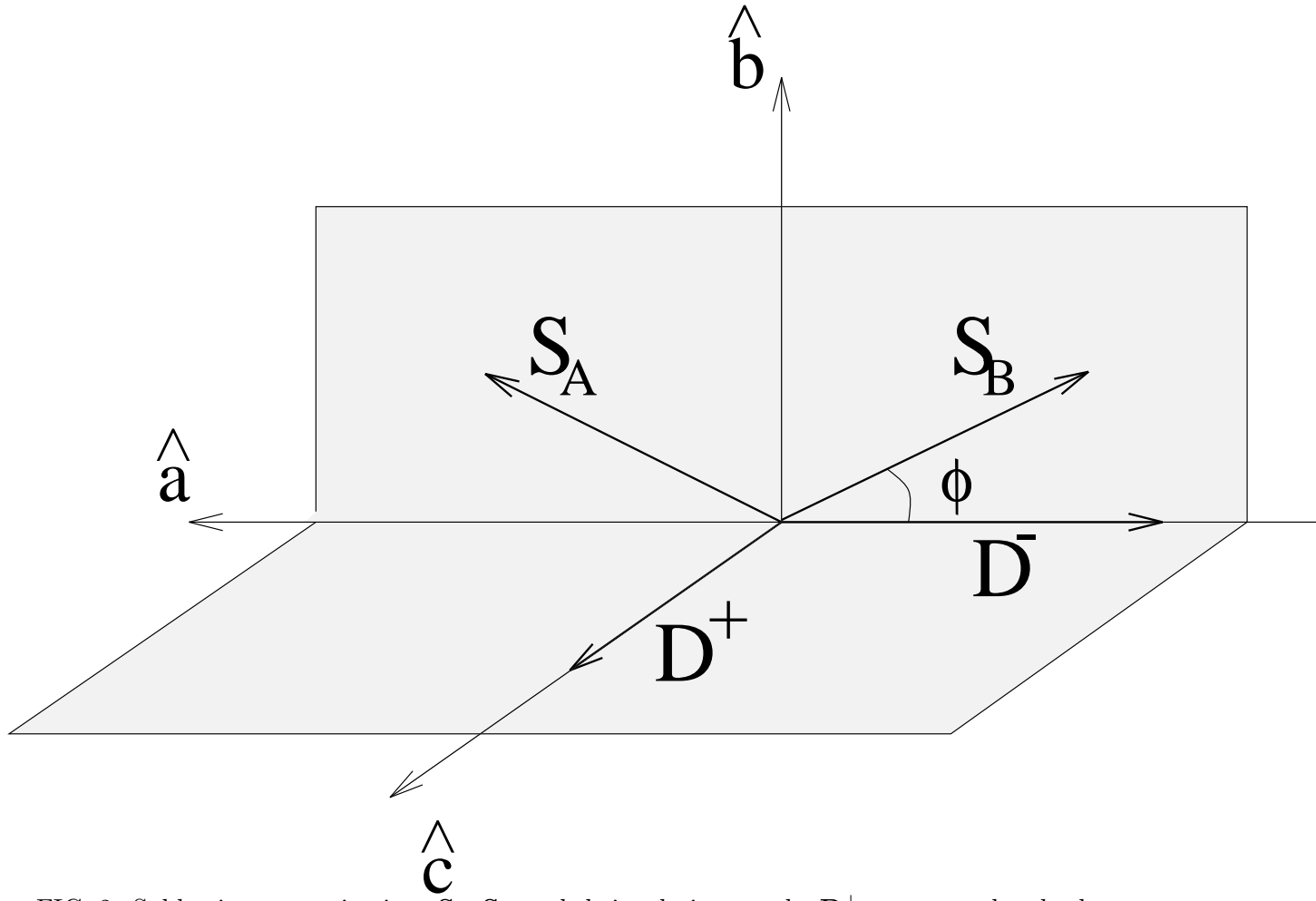


FIG. 2. Sublattice magnetizations  $\mathbf{S}_A, \mathbf{S}_B$  and their relations to the  $\mathbf{D}^\pm$  vectors and orthorhombic axis.

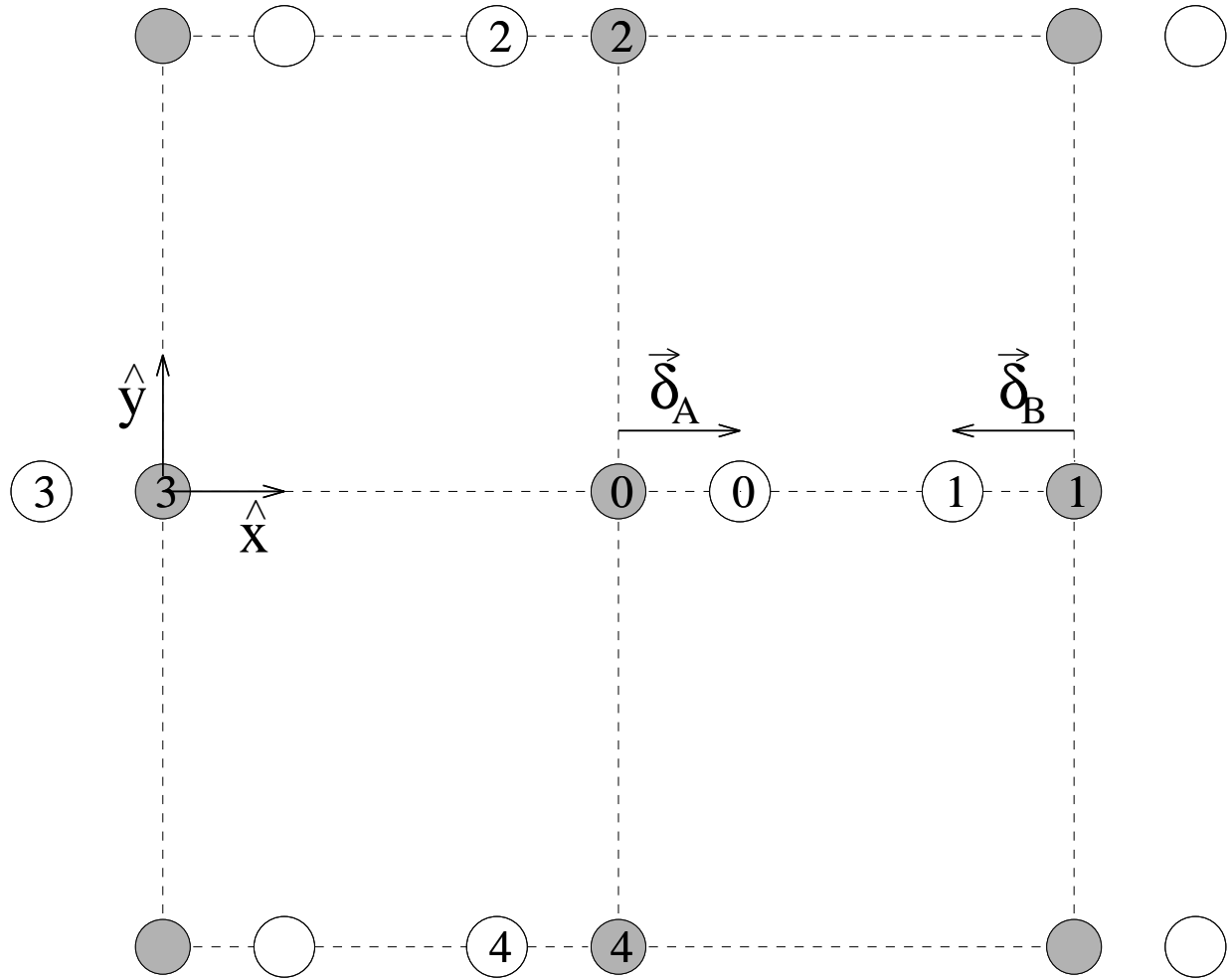


FIG. 3. Displacements of atoms in the  $A, B$  sublattices and the structure of the new decorated square lattice.

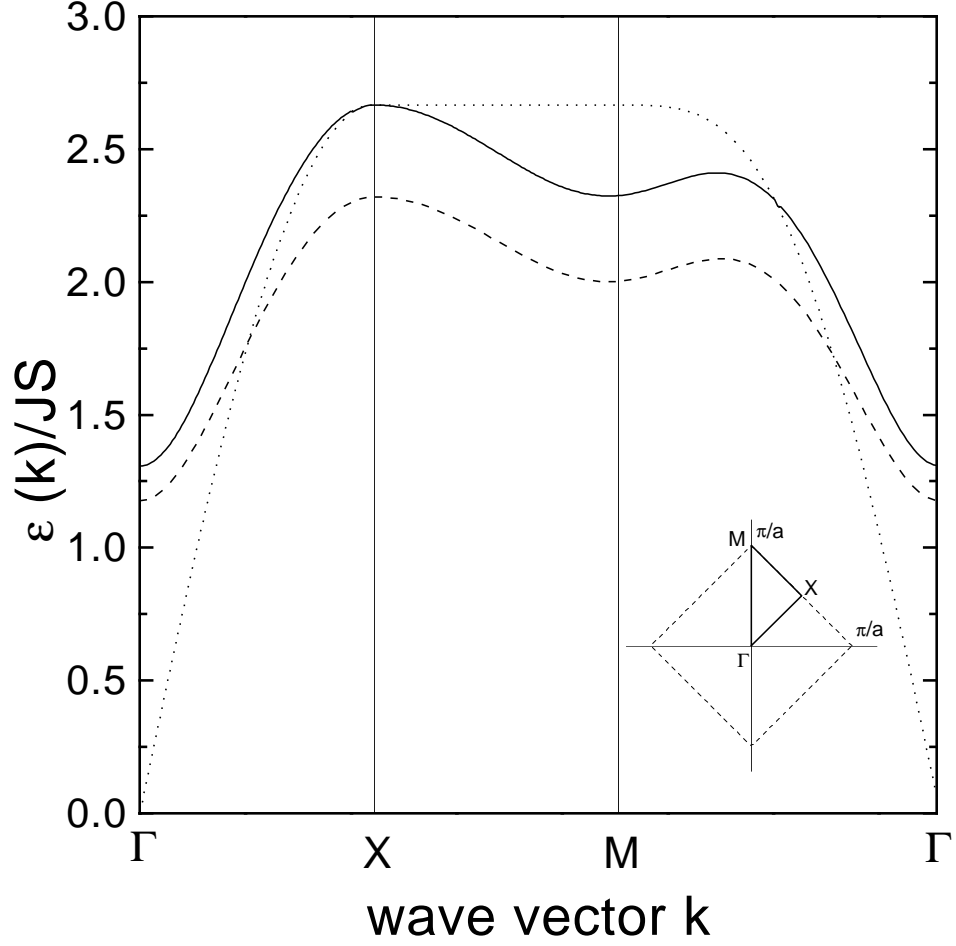


FIG. 4. Quasiparticle dispersion relations for  $r = 0.4$  and  $\beta = 0$ , along the  $\Gamma - X - M$  path shown in the inset. The full line is the Schwinger-boson result for the degenerate gapped branch; the dashed line indicates the linear spin-wave prediction for comparison. The dotted line gives the degenerate gapless branch discussed in the main text.

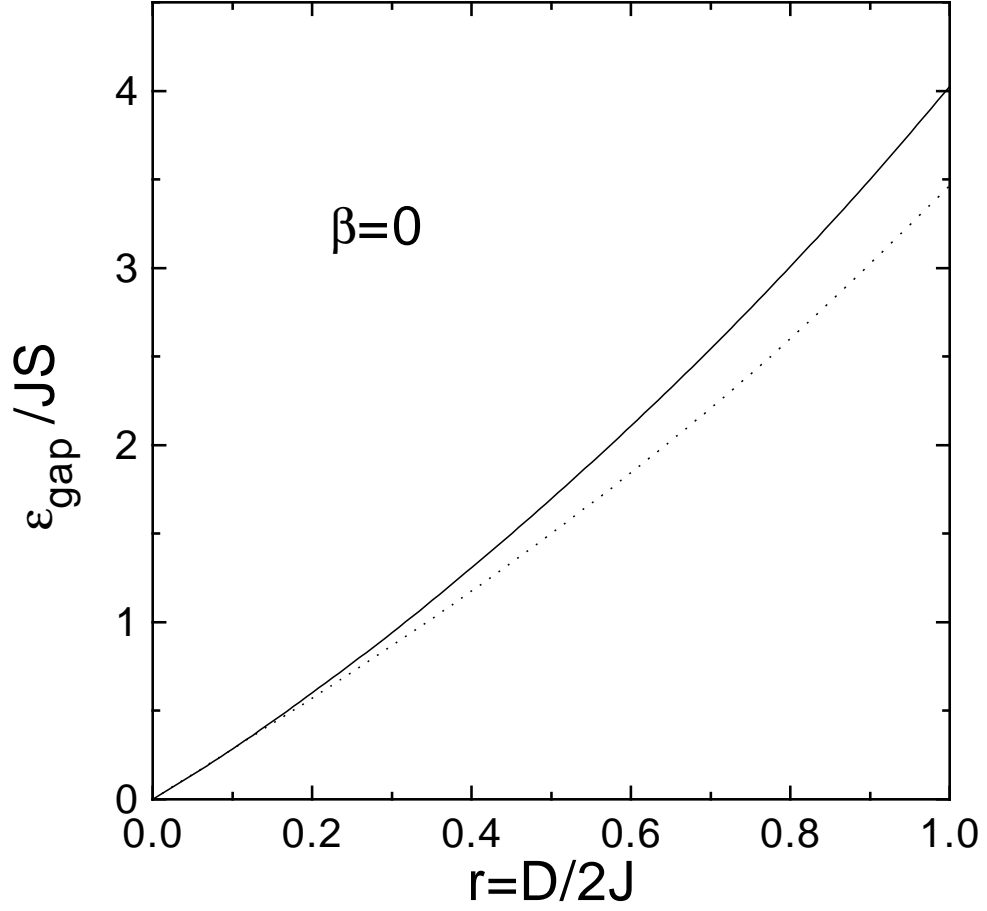


FIG. 5. Anisotropy gap as a function of  $r$  for  $\beta = 0$ . The full line is the Schwinger-boson prediction; the point line gives the linear spin-wave result for comparison.

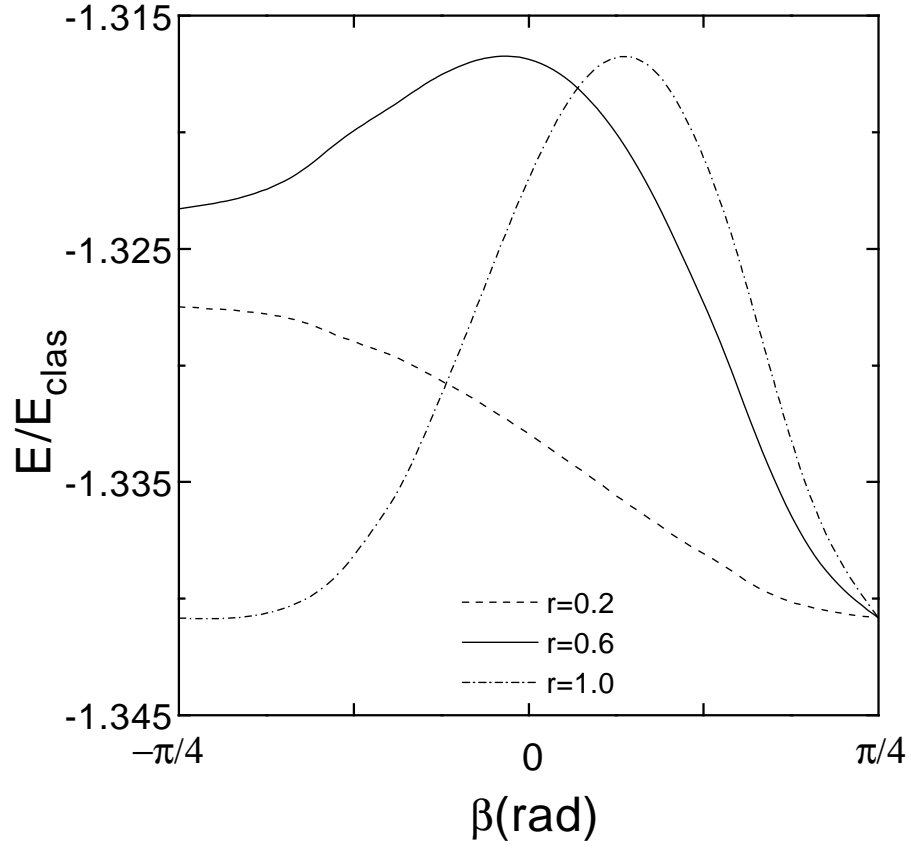


FIG. 6. Ratio between classical and quantum ground-state energies as a function of  $\beta$  for different values of  $r$ .

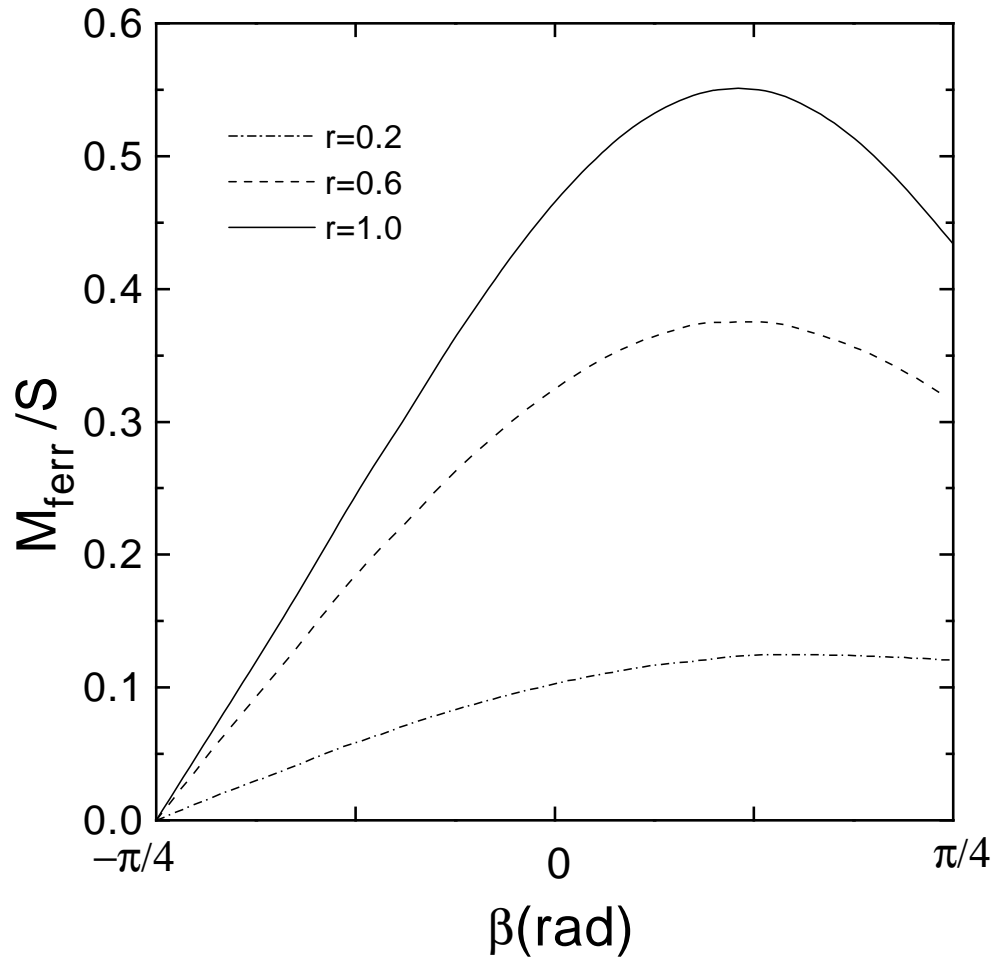


FIG. 7. Net ferromagnetic moment as a function of  $\beta$  for different values of  $r$ .



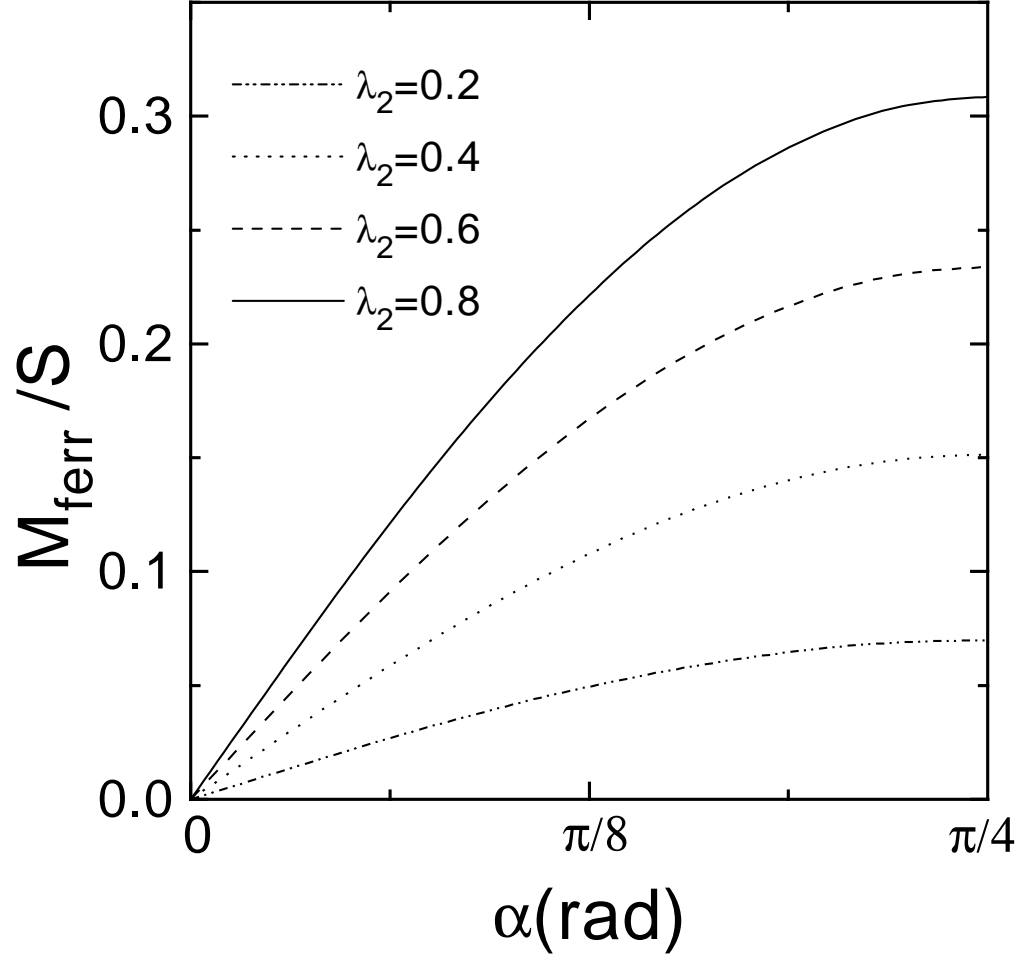


FIG. 8. Net ferromagnetic moment as a function of the direction of the octahedra tilting axis. See the main text for the definitions of the parameters involved.

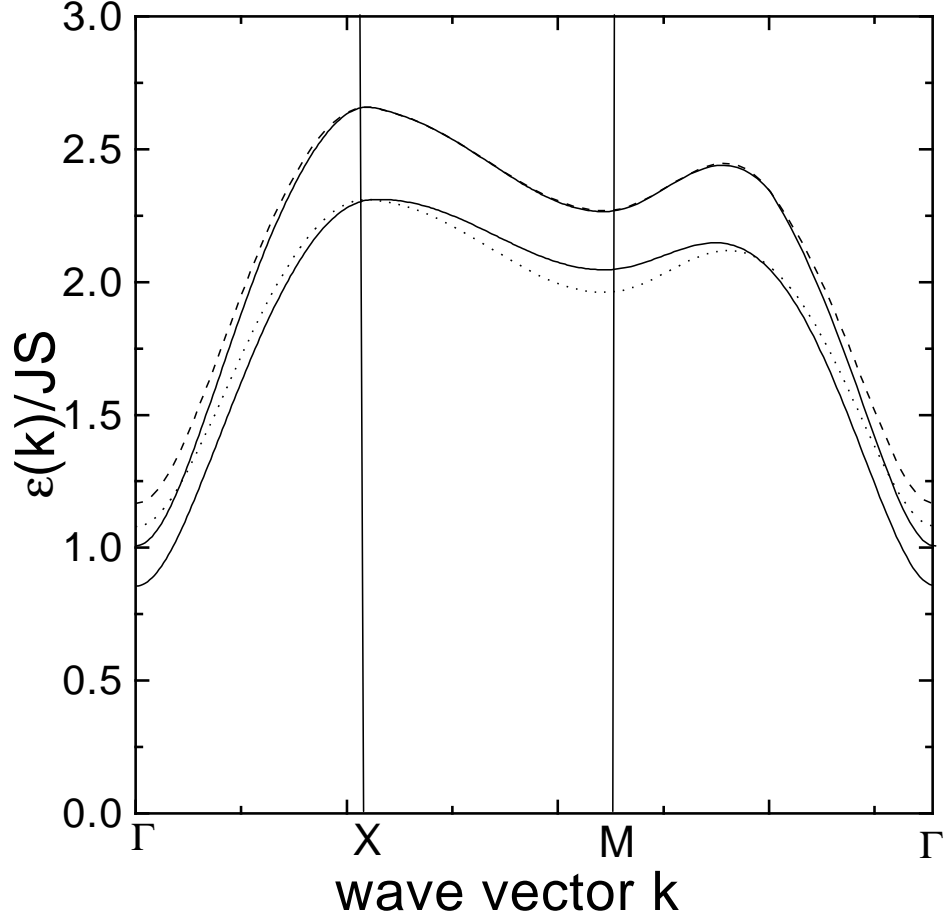


FIG. 9. Splitting of the degenerate gapped quasiparticle branches for  $\Omega = 0.4$ . Upper full and dashed lines: Schwinger-boson results. Lower full and point lines: linear spin-wave predictions.

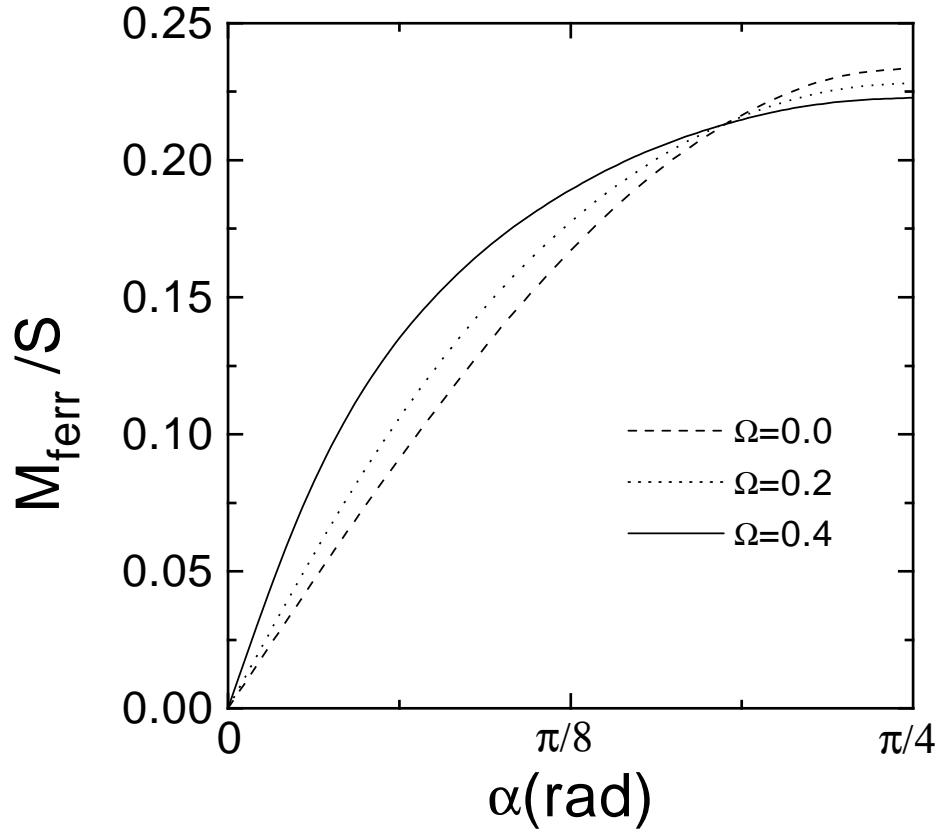


FIG. 10. Net ferromagnetic moment as a function of the direction of the octahedra tilting axis for different values of  $\Omega$ .